Active Damping of a Hydrostatic Steering Circuit for an Articulated Vehicle

Olesen, Emil Nørregård; Andersen, Torben Ole; Ennemark, Poul

Published in:
Proceedings of the ASME 2022 Symposium on Fluid Power and Motion Control

Publication date:
2022

Document Version
Accepted author manuscript, peer reviewed version

Proceedings of the ASME 2022
Symposium on Fluid Power and Motion Control
FPMC2022
September 14–September 16, 2022, Bath, UK

FPMC2022-89927

ACTIVE DAMPING OF A HYDROSTATIC STEERING CIRCUIT FOR AN ARTICULATED VEHICLE

Emil N. Olesen[1,†,*], Torben O. Andersen[2,†] Poul Ennemark

[1]Danfoss Power Solutions, Nordborg, Denmark
[2]AAU Energy, Aalborg, Denmark
[1]Danfoss Power Solutions, Nordborg, Denmark

ABSTRACT

This paper investigates the steering performance of an articulated vehicle with a hydrostatic steering circuit, where the objective is to evaluate the steering performance and comfort level of the vehicle with and without active damping. The steering system is based on a hydraulic actuated system, which response often is underdamped. The operator of such a vehicle is placed on top of the articulation point and the hydraulic cylinders, which then directly translates the underdamped cylinder oscillations into undesired lateral motion of the operator. Active damping is therefore a promising concept for increasing the comfort level of the hydraulic steering circuit.

Keywords: Orbital Steering Unit, Nonlinear Control System, Disk Margin, Relative Stability margins

1. INTRODUCTION

Orbital Steering Pumps (OSP) [1] has been used in articulated vehicles for a long period, as power steering systems. These units functions as a closed loop control system, with the input being the rotation of the steering wheel and corresponding output being the linear movement of a hydraulic cylinder(s).

Despite a relatively simple steering setup, there exist a few cons with this steering circuit. The combination of the steering geometry, loading configuration and that fluid power systems are inherently nonlinear and typically suffer from very poor damping, is causing some problems regarding underdamped oscillations of the steering system in some operations of the vehicle [2]. In the case with a articulated vehicle, for articulated frame steering, the operator is typically placed on top of the articulation point. This means that underdamped cylinder oscillations directly translates into undesired lateral motion of the operator [3] as illustrated in figure 1.

FIGURE 1: Yaw motion of an articulated frame steering vehicle during steering manoevres, resulting in lateral movement of operator.

The problem with these oscillations or underdamped responses is often linked to socalled steering jerks [2], which is a jargon for the physical phenomena called jerk, that describes the dynamic behavior of an acceleration change for a given object with magnitude and direction [4]. These jerks are felt by the operator in situations with a quick transition in acceleration, for example at fast step inputs or steering stops.

[†]Joint first authors
[*]Corresponding author
Documentation for `asmeconf.cls`: Version 1.26, April 19, 2022.

Before a introduction to how active damping can be implemented and investigated, a short description of the orbital control system is introduced in the following with reference to figure 2. The control system has a proportional regulator, which gain is nonlinear.

At the figure a exploded view is shown, the spool is in a application attached to a steering column through a spline connection. This spool and column is able to rotate in the housing together with the sleeve and gearset. The spool and column achieves a input from the operator, and will thereby follow the operators desired trajectory for steering. In the meantime the sleeve and gearset will not follow the spool immediately, because of the spring package, it needs a small relative deflection between the spool and sleeve before the sleeve and gearset starts to rotate. This relative angle works with the same analogy as an error in a closed loop control system, where the mechanical feedback is the sleeve and gearset angle. This means that the spool angle will be ahead of the sleeve and gearset angle, which in the system can be related to the small delay between operator input and wheel rotation.

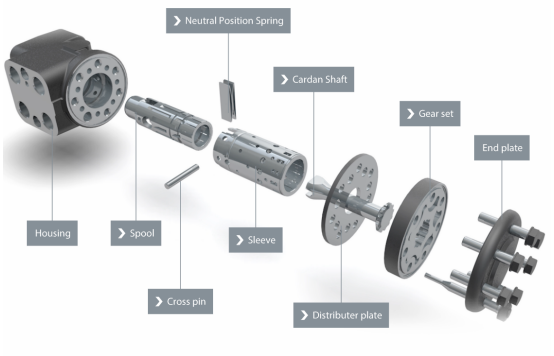

FIGURE 2: Exploded view of a orbital steering unit (OSP).

To avoid these underdamped responses, it is necessary to introduce damping to the system. An Orbital Steering Unit, has a mechanical feedback which limits damping possibilities to being passive. Here different approaches can be mentioned for example wide angle technology and cylinder dampening [2]. A well known technology for introducing damping is active damping [5], and it is therefore interesting to analyze if this can be implemented and which influence it will have on the system performance.

A steering system is though not so straight forward for applying active damping due to functional safety, which requires that the system is safe to operate in all possible situations at all times. However, it is possible to compensate the system with active damping in different ways [5]. In this paper the focus will be on pressure feedback compensation, where the objective will be to compensate the metered flow from the steering unit to the cylinder ports depending on the load pressure from the cylinders. This type of compensation is shown in figure 3 with a block diagram.

The pressure compensation that will be investigated in this paper is a Pressure Gradient Feedback, which only compensates while a transient response occurs on the servo load pressure. In practice it is however not always possible to implement a gradient

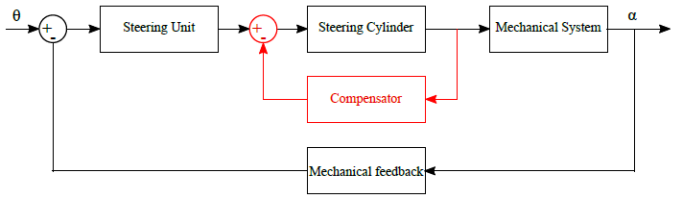

FIGURE 3: An illustrative block diagram of the cascade system for the hydrostatic steering circuit, with an outer position control (OSP) and a internal pressure compensation marked with red.

based feedback alone, due to signal noise problems. Instead it can be considered in combination with either a high pass filter (1) or a band pass filter (2).

$$G_f(s) = \frac{K_f\, s}{\tau_f\, s + 1} \tag{1}$$

$$G_f(s) = \frac{K_f\, s}{(\tau_f\, s + 1)^2} \tag{2}$$

The paper will investigate and evaluate a gradient based feedback compensation, on a specific articulated vehicle located at the Application and Development Center in Nordborg Denmark (Danfoss Power Solutions). The remaining paper will cover this in the following sections:

- Establishment of Time Domain Model
- Verification of Model
- Gradient Based Pressure Compensation
- Field Test of Active Damping

The articulated vehicle utilized, shown in figure 4, is a Terex L310 17.6 Ton wheel loader, which is mounted with measurement equipment.

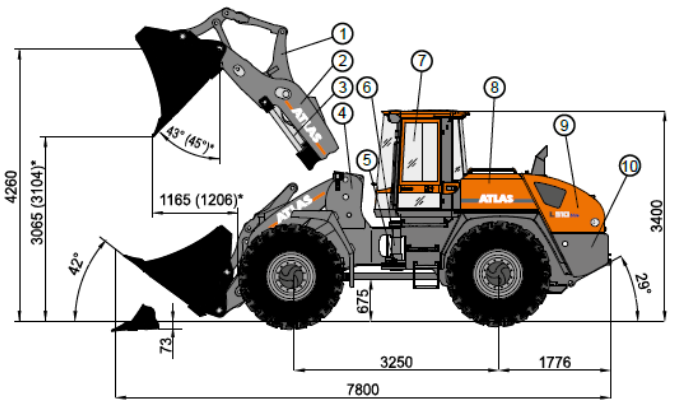

FIGURE 4: An illustrative picture of the Terex L310.

2. TIME DOMAIN MODEL

This section will describe the steering setup for the Terex L310, which consist of a LS pump, a static priority valve, a static OSPUL steering unit, two asymmetric steering cylinders and the mechanical system of the loader. In the following the analytical relations are derived for the system, which is shown in figure 5. A deeper description of the model can be found in the reference [6].

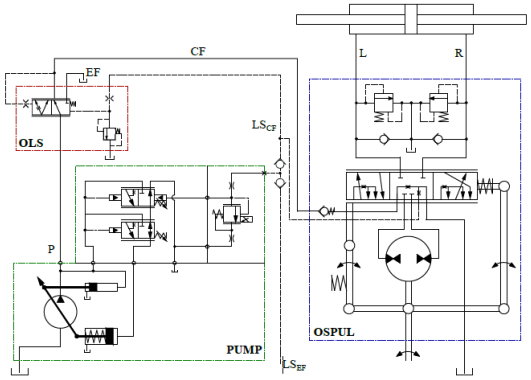

FIGURE 5: Hydraulic diagram of the steering system.

The hydraulic pump is a Danfoss Series 45 frame E pump [7], which is a piston pump with load sensing and variable displacement. The model of this is here omitted, because an existing model was provided from Danfoss.

2.1 Priority Valve

The Static OLS 160 [1], is a flow compensator for the steering unit, which regulates the flow from the pump towards steering circuit and working hydraulics. The priority valve regulates the amount of flow depending on the LS signal from the steering unit, which ensures that the steering circuit is prioritized over the working hydraulics.

The priority valve consist of a combined mechanical and hydraulic system, where the mechanical movement of the internal spool controls the opening towards steering (CF) port and working hydraulics (EF) port. The hydraulic system, shown in figure 6, can be described with the orifice equation (3), and the continuity equation (4).

$$Q_i = C_d\, A \sqrt{\frac{2}{\rho}\Delta P} \tag{3}$$

$$Q_{in} - Q_{out} = \frac{dV}{dt} + \frac{V}{\rho}\frac{dp}{dt} \tag{4}$$

The valve dynamics of the mechanical spool internally, can be described with newtons second law (5), where the force equilibrium is shown in figure 7. The F_{pp} is the pressure point p_{pp} working on the spool area against the pressure force F_{ls}, the friction from the oil film F_μ, flow forces F_{fl} and the margin spring F_k.

$$\ddot{x_v}\, M_v = F_{pp} - F_{LS} - F_{fl} - F_k - F_\mu \tag{5}$$

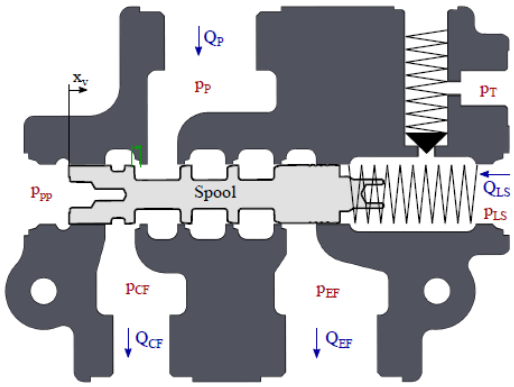

FIGURE 6: Sketch of the inside of the priority valve and hydraulic connections.

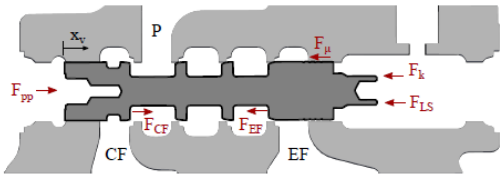

FIGURE 7: Free body diagram of mechanical spool priority valve.

2.2 OSPUL unit

Second component is working as described in the introduction 1. Again here the system consist of a hydraulic part and a mechanical part. The hydraulic system is shown in figure 8, and can be described with the same equations as for the priority valve, the continuity equation (4) and orifice equation (3).

The valve dynamics of the OSPUL unit depends on the mechanical system, which is illustrated with a free body diagram in figure 9. A description of the torques introduced while steering is described in the following, and expressed with equation 6 and 7.

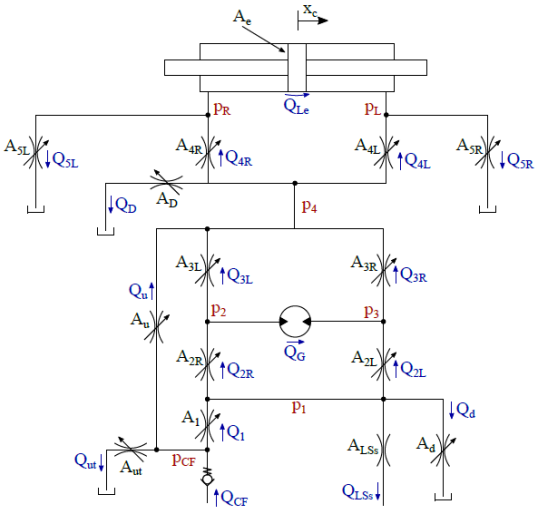

FIGURE 8: Hydraulic model illustration of OSPUL.

$$J\,\ddot{\theta} = \tau(t) - k(\phi)(\theta - \theta_1) \tag{6}$$

$$J_1\,\ddot{\theta_1} = \tau_M(\phi) - \tau_\mu(\dot{\theta_1}) - k(\phi)\,(\theta_1 - \theta) \tag{7}$$

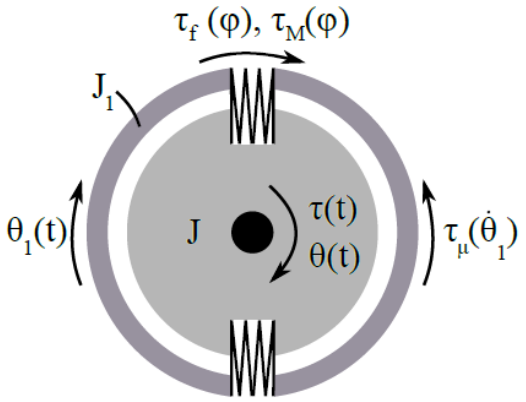

FIGURE 9: Free body diagram of the mechanical system of OSPUL.

When the steering wheel is turned a steering torque $\tau(t)$ is applied at the steering wheel, which results in a acceleration of the spool and steering column inertia (J) and a elastic deformation of the rotational spring (ϕ). Simultaneously with this a spring torque (τ_f) will be applied to the sleeve and gearset together with a hydraulic motor torque (τ_M) from the gear set which will depend on the slip angle. The resulting torque from these two contributions will be transferred into a acceleration of the inertia of the sleeve and gearset (J_1) which is affected of a opposite acting friction torque (τ_μ).

2.3 Cylinder and Mechanical System

Third component is the steering geometry and mechanical system of vehicle, the purpose here is to transfer the cylinder force from the steering cylinder into the movement of the steering mechanism, where the output is the steering angle of the vehicle. The mechanical model is modelled with the use of Lagrange equation, which is generally described with equation (8).

$$\frac{d}{dt}\frac{\partial T}{\partial \dot{q}} - \frac{\partial T}{\partial q} + \frac{\partial V}{\partial q} = Q_y \tag{8}$$

where $q = \{\alpha\}$ and $\dot{q} = \{\dot{\alpha}\}$

The vehicle is here considered as a rigid multi body system, where it is possible to describe it from a 2D perspective. Secondly the two asymmetric cylinders shown at figure 10, is summed to one symmetrical one instead. At the figure the kinematic relationship between cylinder movement and vehicle rotation is also visualised.

The kinetic energy of the system depends on the inertia which is calculated with a CAD assembly of the vehicle, where the inertia is taken around the articulation point. The external forces considered for the system is friction from the tires together with the torque from the cylinders.

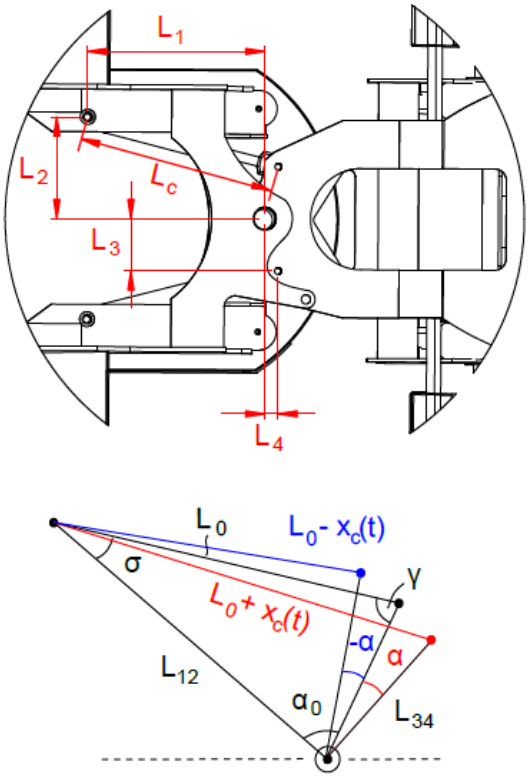

FIGURE 10: Figure for kinematic relationship of wheel loader.

The tyre modelling is here done with a simplified hysteresis model, where the lateral motion of the tyre will initially be an elastic deformation of the tyre until eventually the tyre will slide. This behavior is converted to a torque around the articulation point and described in the following points together with the illustration shown in figure 11.

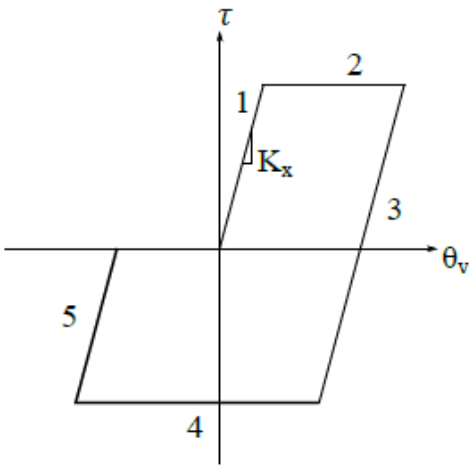

FIGURE 11: Hysteresis model showed using an example, where the vehicle initially rotates to the right and afterwards to the left.

1. The vehicle rotates to the right, and the tyres deform elastically.

2. The vehicle continues to rotate to the right, but the tyre is sliding, and therefore, the tyre torque has reached saturation.

3. The vehicle rotates to the left. The tyre deformation is initially relieved until it is deformed in the opposite direction and introduces a torque in the opposite direction.

4. The vehicle continues to rotate to the left, but the tyre is sliding, and the torque has reached saturation.

3. VERIFICATION OF MODEL

In this section a verification of the derived model of the system will be covered, where vehicle test on the wheel loader will be evaluated and compared. The dynamics of the system is of great concern here, especially the R and L pressure behavior, because these represent the behavior of the states that is intended to control with the pressure compensation strategy.

The experimental test will be used to evaluate hard parameters, which could be spool mass, moment of inertia, volumes and area curves. While more soft parameters, which is more difficult to obtain, is fitted with an optimization routine. These soft parameters are for example friction coefficients.

3.1 Wheel Loader Test

The wheel loader test is done with a steering robot, which is capable of producing many different steering inputs. The torque from this robot is here limited to 5 Nm, because this point will give a steering velocity of approximately 120 RPM.

Three different test sequences is done with the robot:

1. Velocity Step input of 20 RPM
2. Velocity Step input of 40 RPM
3. Random Binary Sequency of Steering velocity

It is chosen to focus on the pressure points P_R and P_L in the evaluation. The first test results and comparison between model and measurements are shown in figure 12. Second test is shown in figure 13, and finally the third test is shown in figure 14.

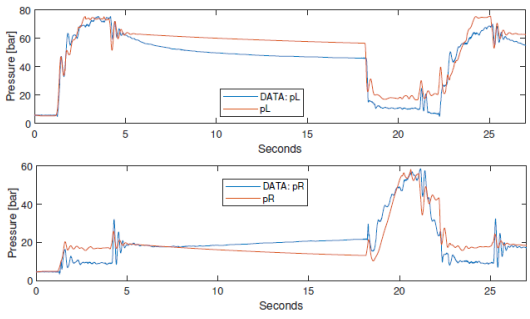

FIGURE 12: Step 20 RPM: Orange is model output, and blue is experimental data.

For the first step input there is a deviation in the steady state pressure level, but in general most of the pressure oscillations amplitude and frequency is replicated with the model. Especially at approximately 4 and 24 seconds, where both step input stops, here there is a good correlation between pressure oscillations.

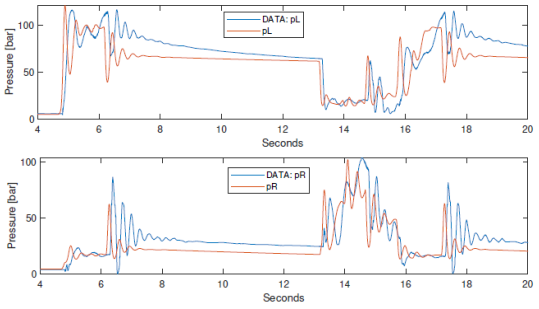

FIGURE 13: Step 40 RPM: Orange is model output, and blue is experimental data.

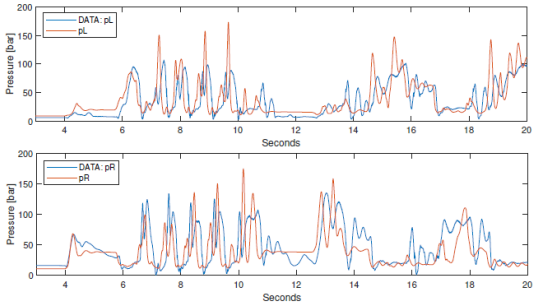

FIGURE 14: Random Sequence: Orange is model output, and blue is experimental data.

For the second step input, the oscillations is deviating with an offset in time, and amplitude. The model oscillations initiates faster, but looking at the frequency similar tendencies are displayed and is correlating.

For the random input, the offset and amplitude deviation is again present, but again with a correlation between frequency of model and measurements. In general it is assessed that the model can be used to develop control algorithms as it captures the essential pressure dynamics of the system. Hence it is presumed that if the control algorithm can reduce pressure oscillations on the model, it will also work on the real system. However, it must be robust and/or adaptive to changing conditions, because model and experimental test differs from one input to another, which indicates that the dynamics is quite sensitive to input type.

4. GRADIENT BASED PRESSURE COMPENSATION

The objective for the controller, is to dampen the motion of the cylinder without compromising the steady state gain of the system too much, which is achieved by adjusting the metered flow for the cylinder in the right frequency interval depending on the pressure transients of the servo load. It is difficult to obtain hard requirements for the responsiveness and steady state error that the controller should obtain, because the steering feeling of the vehicle is felt individually depending on the operator and application.

Pressure feedback can be introduced in the system as visualised with block diagram 3, where the actuator for this compensation type in this case is an EHi valve [8], which works as a 4/3 servo valve shown in figure 15.

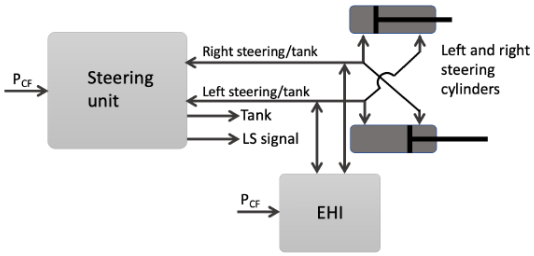

FIGURE 15: Schematic of the connection between the EHi and the steering unit.

This actuator can then adjust the metered flow to the cylinder from the steering unit, which will be controlled actively depending on pressure sensors on the P_R and P_L ports visualised with figure 16.

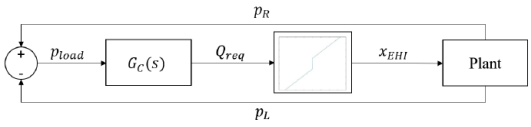

FIGURE 16: Block diagram of the actuator compensation.

In this case the controller G_c will be a gradient based pressure feedback controller with a high-pass filter introduced, equation (9), to ensure high frequent signal noise is avoided. The objective is here to design a gain K and break away frequency for the high pass filter that matches the system dynamics of the Terex steering system. Traditionally this is done by examining a linear plant model, and therefrom theoretically place the pole position of the high-pass filter and determine the gain value. But due to a very nonlinear model with very sensible parameters it is instead chosen to use the nonlinear model as reference, and then tune the parameters to obtain a desired performance by evaluating pressure behavior and cylinder position depending on step inputs.

$$G_c = K \frac{\omega s}{s + \omega} \tag{9}$$

Depending on the inertia of the vehicle, empty vs loaded bucket, the pressure oscillations has a frequency in the area from 2.5 Hz to 4 Hz. Initially a fixed breakaway frequency is used for the high-pass filter, where the controller impact on the system will depend on the placement of the pole. The break frequency of the high-pass can be chosen to be either below, equal to, or above system eigenfrequency, which is shown in figure 17. Due to the zero in the high pass filter, a phase lead is introduced, which is cancelled by the pole at higher frequencies. Assuming the load pressure oscillates at the eigenfrequency ω_n the high-pass filter will introduce a phase lead with an angle that depends on the eigenfrequency and the break frequency of the filter. The lead effect can be utilised to compensate for the lag effect in the electrohydraulic valve dynamics, and thus, it may be an advantage to choose a break frequency that is equal to or above the eigenfrequency of the system.

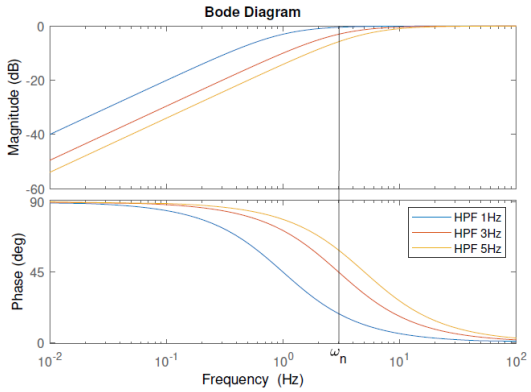

FIGURE 17: Bode Plots of high-pass filters with different break frequencies.

The valve dynamics for the EHi is introduced in the nonlinear model through a second order system with a eigenfrequency of 8 Hz and a damping ratio of 1. With this implementation different controllers are tested in the nonlinear model, where three designs are compared without active damping control in figure 18.

The same proposed controllers will be evaluated during field test on the wheel loader, where different tests with the steering robot with and without active damping will be analyzed. This will be covered in the next section regarding field test.

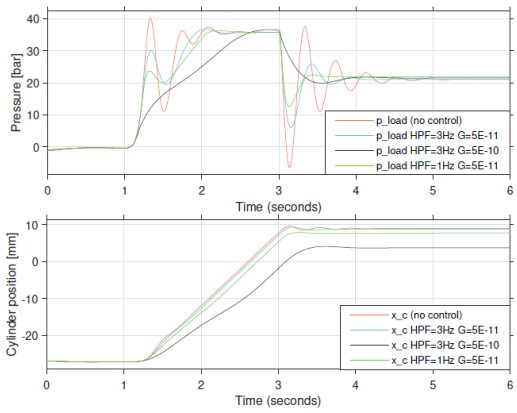

FIGURE 18: Model simulations of load pressure and cylinder position with and without pressure feedback.

5. FIELD TEST OF ACTIVE DAMPING

In this section, the field test will be covered, where a comparison for steering performance with and without active damping is done. To be able to analyze and prove the change in comfort for the operator, an evaluation is done accordingly to the ISO standard 2631-1. This standard is a procedure for how to evaluate the effect of vibrations exposed to the human body.

For the case with the Terex wheel loader, all accelerations from the cab was measured, in sex degree of freedoms, for each test with and without active damping for the same input. The interesting acceleration in this case is the lateral acceleration of the seated operator, which is visualised in figure 19 in the y-axis

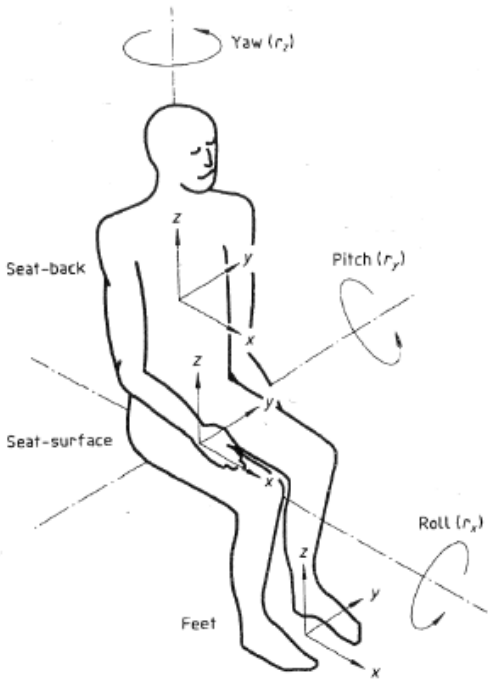

FIGURE 19: ISO standard for acceleration direction alignment.

direction. This acceleration is treated by two different weighting methods, described in the standard.

First method is an evaluation of the vibrations based on the RMS value of the acceleration, which is expressed with equation 10. Where a_w(t) is the weighted acceleration and T the duration of the measurement.

$$RMS = \sqrt{\frac{1}{T}\int_0^T a_w^2(t)dt} \tag{10}$$

Second method is a running RMS value, which is used if the accelerations are peaking rarely and the vibrations thereby are underestimated with the first method. This evaluation is called RRMS and is expressed with equation 11. Here τ is integration time for running averaging and t_0 is the instantaneous time.

$$RRMS(t) = \sqrt{\frac{1}{\tau}\int_{t_0-\tau}^{t_0} a_w^2(t)\,dt} \tag{11}$$

From initial measurements on the wheel loader it is concluded that RMS is not sufficient enough alone, due to a ratio of the measured acceleration profile. Therefore both RMS and RRMS values are used to evaluate the vibrations and the quality of the implemented damping.

The test procedure is done with three different inputs, first input is a pin to pin test, where two fast turns (100 RPM) on the steering wheel are given as input, one to each side. Second input is a quarter to pin test, where a right turn of a quarter of a rotation is given with medium velocity (50-60 RPM) followed by an abrupt stop. The third test is a slip test, where a full rotation to right or left is performed followed by a short break, such that the system can settle, then ending with a full rotation back again.

These three inputs are used to test the active damping influence on both oscillations, steering responsiveness and slip between operator input and cylinder movement. A total of 20 test was performed, where different controllers has been evaluated and different bucket loading's of the wheel loader has being tested. In table 1, the different gain and high-pass filter frequencies is noted together with a calculated average effect of the active damping. The table consist of the best performed tests, where an improvement of more than 40 % is shown, which clearly indicates that the active damping concept works as intended.

Test	Load	K	ω	Ave. Damping
3	Yes	5E-11	3 Hz	44,51 %
9	Yes	5E-11	3 Hz	52,75 %
13	Yes	7,5E-11	3 Hz	50,27 %
14	Yes	7.5E-11	5 Hz	49,16 %
16	Yes	5E-11	5 Hz	39,70 %
19	Yes	5E-10	5 Hz	53,9 %
20	Yes	5E-11	1,5 Hz	56,22 %

TABLE 1: List of performed test, with notation of gain, break frequency, loading and average effect of active damping.

6. CONCLUSION

The objective of the paper was to examine an articulated vehicle with a hydrostatic steering circuit, where the steering performance and comfort level of the vehicle with and without active damping should be analyzed.

From this analysis it can be concluded that an nonlinear model is derived and verified, which enables to replicate the dynamic response of the steering circuit for the Terex Wheel loader.

The nonlinear model is utilized to develop a gradient based pressure compensation, which actively dampens the steering system depending on the servo load pressure.

The active damping strategy is implemented on the wheel loader, where the actuation is done by a EHi valve. It can here be concluded from field test that the active damping method is able to reduce under damped vibrations with at least 40 %.

ACKNOWLEDGMENTS

Place any acknowledgments here.

REFERENCES

[1] Solutions, Danfoss Power. "OSPB/C/F/D/L LS, OLS Priority Valves, OSQ Flow Amplifiers." Technical datasheet -. Danfoss, Nordborg, Denmark. 2019. URL http://hdl.handle.net/-.

[2] Reitz, Mark. "A Systems Approach to Smooth Steering." *OEM Off-Highway* URL https://www.oemoffhighway.com/home/article/10166537/a-systems-approach-to-smooth-steering.

[3] Olesen, Emil Nørregård. "Active damping of a hydrostatic steering circuit, for an articulated vehicle." Master's Thesis, Aalborg University, Aalborg, Nordjylland. 2020.

[4] David Eager, Nina Reistad, Ann-Marie Pendrill. "Beyond velocity and acceleration: jerk, snap and higher derivatives." *European Journal of Physics* URL https://iopscience.iop.org/article/10.1088/0143-0807/37/6/065008.

[5] R. Rahmfeld, M. Ivantyssynova. "An overview about active oscillation damping of mobile machine structures." - .

[6] Lindrup, Jens and Soele, Jesper. "Active damping of a hydrostatic steering circuit, for an articulated vehicle." Master's Thesis, Aalborg University, Aalborg, Nordjylland. 2021.

[7] Solution, Danfoss Power. Technical report no.

[8] Danfoss. *Operation manual PVED-CL Controller for Electro-Hydraulic Steering Version 1.38* (2020).